Growth phase influences virulence in *Candida auris* systemic infection models

Michael J. McFadden, Juliet A.E. Anku, Faith A. Davis, Teresa R. O'Meara[†]

Affiliations:

Department of Microbiology and Immunology, University of Michigan, Ann Arbor, MI 48109, USA.

[†] Corresponding author: Correspondence to Teresa R. O'Meara (tromeara@umich.edu)

Abstract

Candida auris is a growing public health concern, capable of causing long-term contamination of healthcare settings, skin colonization, and life-threatening bloodstream infections. However, *C. auris* pathogenesis is not well understood, which is exacerbated by limitations and discrepancies in existing animal infection models. Further, the effects of *C. auris* growth phase on virulence have not been examined, despite growth phase being linked to virulence in many bacterial species. To address this question, and to develop an immunocompetent murine model of infection, we directly compared log and stationary phase *C. auris* systemic infection in immunocompetent C57BL/6J mice at high and low doses of infection. Systemic infection with high dose log-phase *C. auris* results in rapid mortality between 2 hours and 1 day post infection, whereas stationary phase *C. auris* results in significantly extended survival. However, at low doses of infection, there was no difference in mortality kinetics between log and stationary phase cells. We observed that *C. auris* initially colonizes multiple organs but is rapidly cleared from the lungs and spleen, while kidney fungal burdens remain stable. Decreased fibrinogen levels and blood clotting in the lungs of mice infected with high dose log-phase *C. auris* suggest that blood clotting may drive rapid mortality, potentially associated with increased β-glucan exposure and mannan abundance observed in log phase *C. auris*. These results will inform the development of a more standardized animal model of systemic *C. auris* infection, which can be used to reveal key aspects of *C. auris* pathogenesis.

Importance

Despite its growing medical importance, there is limited understanding of *Candida auris* pathogenesis, due in part to limitations of existing laboratory models of infection. To develop a more complete understanding of factors that contribute to *C. auris* pathogenesis, it will be

34 necessary to establish consistent parameters for animal models of infection. To address this need,
35 we directly compared log and stationary growth phases on *C. auris* pathogenesis in
36 immunocompetent C57BL/6J mice using a single Clade I isolate. At a high dose of infection, host
37 survival was dramatically different between log or stationary phase *C. auris*, suggesting that
38 growth phase can affect *C. auris* virulence. These differences correlated with increased exposure
39 of pathogen-associated molecular patterns in the *C. auris* cell wall in log phase cells. These
40 results will be instrumental in the future development of standardized animal models to study *C.*
41 *auris* pathogenesis.

42

43 **Introduction**

44 *Candida auris* is an often multidrug resistant invasive species within healthcare settings
45 that also can cause systemic infection with mortality rates higher than 30% (1, 2). *C. auris*
46 pathogenesis is not well understood due to its recent emergence and the existence of
47 comorbidities in many infected patients, as well as an incomplete understanding of host-pathogen
48 interactions and pathology within sites of *C. auris* infection (3–5). While animal models have been
49 of great utility in understanding the relative contribution of specific fungal mutants to virulence (6–
50 9), there is not a standard animal model for *C. auris* disseminated disease. The
51 immunocompromised model of *C. auris* was initially developed as a physiologically relevant model
52 of systemic infection, with a particular focus on its utility for testing of antifungal compounds (10)
53 or specific types of immunocompromise (11). Immunocompetent models of *C. auris* infection have
54 also been developed in ICR outbred mice (12), BALB/c (13), and C57BL/6J (3, 4) backgrounds,
55 with varying kinetics and rates of mortality. Additionally, *C. auris*-specific factors, such as strain
56 background are likely a major source of variability between publications as evidenced by our
57 recent work showing significant differences in virulence between two closely related clade I
58 isolates (6). Beyond strain differences, work in bacterial pathogenesis has demonstrated that

growth phase can also influence virulence, but the effects are species specific and were determined empirically. For example, for *Legionella* and *Brucella*, entry into stationary phase is associated with increases in virulence factor expression (14, 15), but for *Salmonella* and *Streptococci*, it is the exponential growth phase that is associated with virulence (16, 17). Therefore, we sought to determine the effects of *C. auris* growth phase and dosage on host survival and pathology using a single strain of *C. auris* and a single genetically tractable and immunocompetent murine model of systemic infection.

At a high dose of systemic *C. auris* infection, we observed that log/exponential phase fungi cause rapid mortality compared to stationary phase fungi, which cause mortality over the course of several days. These differences in mortality may stem from rapid extensive blood clotting caused by log phase *C. auris*, as we observed decreased serum fibrinogen levels and blood clotting in the lungs. Exponentially growing *C. auris* cells had increased β-glucan exposure and mannan abundance, potentially promoting detection by host cells and triggering blood clotting and rapid mortality. However, differences in mortality observed at a high dose of infection were ablated at a low dose of infection, in which mice survived over the course of multiple weeks. We recovered *C. auris* from the lungs, spleen, and kidneys early after infection, but over time, only the kidneys maintained a substantial fungal burden. Together, these results suggest that growth phase can have dramatic effects on survival during systemic *C. auris* infection. Additionally, our work provides new insight into *C. auris* disease progression and will be helpful in establishing more standardized approaches to modeling *C. auris* infection in immunocompetent mouse models.

Results and Discussion

82 **Comparing the Effect of Candida auris Growth Phase on Survival Kinetics and Fungal**
83 **Burden in Organs**

84 To assess whether growth phase affects virulence during systemic *Candida auris* infection,
85 we compared infection outcomes in an immunocompetent murine model using log or stationary
86 phase *C. auris* cultures at a high and low dose of infection ($5x10^7$ and $1x10^6$, respectively) using
87 the AR0382 (B11109 clade 1) isolate (Fig. 1A). Following intravenous infection, each group was
88 monitored for several hours for the onset of disease symptoms. Interestingly, a majority of the
89 cohort infected with a high dose of log phase *C. auris* rapidly declined in health, becoming
90 moribund and showing labored breathing within 2 hours of infection, resulting in humane sacrifice.
91 None of the mice in this group survived beyond the first day post-infection (Fig. 1B). In contrast,
92 mice infected with a high dose of stationary phase *C. auris* survived significantly longer than their
93 log phase-infected counterparts, with onset of mortality starting at day 2 post-infection and full
94 cohort mortality at day 6 post-infection (Fig. 1B). However, at the low dose of infection, we did not
95 observe any significance in mortality between the log and stationary phase infection cohorts (Fig.
96 1C). These data suggest that the growth phase of *C. auris* affects pathogenesis in murine infection
97 models specifically at a high dose of infection.

98 We measured the fungal burden in the lungs, kidneys, and spleen post-mortality in each
99 cohort. In the high dose log-phase *C. auris*-infected cohort, which had very rapid mortality, we
100 observed a significantly higher fungal burden in the lungs than in the stationary phase cohort,
101 while there was no difference in burden in the kidneys or spleen (Fig 1E, F). However, the
102 difference observed in lung fungal burden is likely a product of survival kinetics, rather than
103 colonization, as the fungal burden in the lungs appeared to sharply decrease over time (Fig. 1G).
104 In low dose cohorts, which survived significantly longer than high dose cohorts, we recovered
105 very few fungal colonies from the lungs, indicating that *C. auris* is effectively cleared from the
106 lungs over time (Fig. 1J).

107 Similarly, fungal burden in the spleen showed a decreasing trend at day 7 in the high dose
108 cohort (Fig. 1H) and was generally low at the time of mortality in the low dose cohorts (Fig. 1K),
109 consistent with clearance from these organs over time. In contrast, fungal burden in the kidneys
110 remained consistent over time in both the high dose (Fig. 1I) and low dose cohorts (Fig. 1L).
111 Together, these data suggest that *C. auris* disseminates to multiple organs after systemic infection
112 but is cleared from the lungs and spleen, while fungal burden remains steady over time in the
113 kidneys.

114 **High Dose Systemic Infection with Log Phase C. auris Causes Rapid Blood Clotting.**

115 We next sought to further understand the differences in mortality observed between log
116 and stationary phase *C. auris* during systemic infection at a high dose. We noted animals that
117 rapidly succumbed within the log phase high dose cohort exhibited blood clotting while performing
118 cardiac puncture, a common feature of sepsis (18). Indeed, ELISA data showed decreased
119 Fibrinogen levels in the plasma of this cohort (Fig. 2A), consistent with Fibrinogen being converted
120 to insoluble Fibrin to form clots (19). Interestingly, levels of proinflammatory cytokines TNF, IL-6,
121 and IL-1β were similar between the log and stationary phase high dose cohorts (Fig. 2B-D),
122 suggesting blood clotting, rather than a cytokine storm, drives rapid mortality after systemic
123 infection with log phase *C. auris*. Blood clots could also be observed in hematoxylin and eosin
124 (H&E)-stained lungs from the log-phase infected cohort (Fig. 2E). Together, these data suggest
125 that rapid blood clotting causes mortality after systemic infection with log phase *C. auris* at high
126 dose.

127 We hypothesized that *C. auris* growth phase may affect the composition of the cell wall, triggering
128 differential recognition and leading to septic shock. Therefore, we measured the major cell wall
129 components chitin, mannan, and exposed β-glucan in log or stationary phase *C. auris*. Flow
130 cytometry analysis revealed that log phase *C. auris* showed higher β-glucan exposure than
131 stationary phase (Fig. 2F, I) and two distinct populations of high and low mannan cells, compared

132 to stationary phase, which showed a single peak with intermediate intensity (Fig. 2G, J). Mannan
133 binding lectin-associated serine proteases can trigger blood clotting (20), revealing one possible
134 mechanism by which the high mannan log phase *C. auris* may trigger rapid mortality at a high
135 dose. In contrast, chitin levels were similar between log phase and stationary phase *C. auris* (Fig.
136 2H, K). These results reveal changes to the composition of the cell wall and exposure of pathogen
137 associated molecular patterns in log phase *C. auris* cells, which may drive the
138 immunopathological response and mortality observed during systemic infection at a high dose.
139 Together this work establishes virulence differences between stationary and log phase *C. auris* at
140 high doses and indicates that the development of a standardized murine infection system,
141 including controlling for fungal growth phase, will be important for future studies examining *C.*
142 *auris* pathogenesis.

143

144

145 **Methods**

146 ***Candida auris* growth conditions.** *C. auris* strain CDC-AR0382 (B11109) was grown in YPD
147 liquid media (1% yeast extract, 2% peptone, 2% dextrose) with constant agitation. After 16 hours,
148 stationary phase cultures were sub-cultured by diluting to OD600 of 0.2 in fresh YPD and grown
149 at 30°C for 4 hours with constant agitation to establish log phase growth.

150

151 **Survival analysis post-systemic infection.** *C. auris* from log phase or stationary phase cultures
152 were pelleted by centrifugation (5000 rpm for 5min), washed once with sterile PBS, and
153 resuspended in sterile PBS to desired doses for infection. Immunocompetent 8-week old female
154 C57BL/6J mice were infected intravenously with *C. auris* from log phase or stationary phase
155 growth at high dose ($5x10^7$) or low dose ($1x10^6$) via retro-orbital injection in 100 µL volume.

156 Immediately following infection, mice were monitored for onset of disease symptoms for several
157 hours initially, then daily over the course of 21 days. Mice were sacrificed at a humane endpoint
158 defined as loss of 20 percent of initial bodyweight, or when severe disease symptoms were
159 observed, such as unresponsiveness and labored breathing, or severe neurological symptoms.

160

161 **Analysis of fungal burden in organs post-mortality.** After sacrifice, organs samples were
162 harvested to measure fungal burden. The right lung, right kidney, and spleen were harvested by
163 dissection and homogenized by bead beating with sterile ⅛ inch ball bearings (Grainger 4RJL3)
164 for 10 seconds. Serial dilutions were performed and plated on YPD agar with ampicillin (100
165 mg/mL) and gentamicin (50 mg/mL). Fungal colonies were grown for 2 days at 30°C and counted,
166 and fungal burdens per organ were calculated.

167

168 **Histological analysis in organs post-mortality.** After sacrifice, organs samples were harvested
169 to perform histological analysis. The left lung and left kidney were harvested by dissection and
170 fixed in 10 percent formalin for 24 hours, then plunged in 70 percent ethanol prior to sectioning
171 and staining (H&E and PAS) by the University of Michigan Orthopaedic Research Laboratories
172 Histology Core. Slides were imaged using a BioTek Lionheart FX automated microscope.

173

174 **ELISA.** After sacrifice, serum was collected by cardiac puncture, followed by isolation of serum
175 using centrifugation (8000g for 5 minutes) of lithium heparin serum collection tubes (Kent
176 Scientific KMIC-LIHEP). Serum samples were submitted to the University of Michigan Cancer
177 Center Immunology Core for quantification of Fibrinogen, TNF, IL-6, and IL-1β by ELISA.

178

179 **Analysis of cell wall content.** Log and stationary phase *C. auris* cells were pelleted by
180 centrifugation (3000 x g for 5 minutes), washed once in PBS, and fixed in 4% paraformaldehyde
181 for 15 minutes. Following fixation, *C. auris* cells were pelleted by centrifugation (3000 x g for 5
182 minutes), washed twice in PBS, and then stained for cell wall contents, followed by flow cytometry
183 analysis. To quantify mannan content, cells were stained with 5 µg/mL of FITC-Concanavalin A
184 (MilliporeSigma, C7642) for 30 minutes. To quantify exposed β-1,3-glucan, cells were blocked
185 with 3% bovine serum albumin & 5% normal goat serum (Invitrogen, 10000C) for 30 minutes.
186 After blocking, cells were stained with 15 µg/mL of hDectin-1a (InvivoGen, fc-hec1a-2) for 1 hour.
187 Cells were washed twice with PBS before secondary staining with 4 mg/mL of goat raised anti-
188 human IgG antibody conjugated with Alexa Fluor 647 (Invitrogen A-21445) for 30 minutes. To
189 quantify chitin content, cells were stained with 0.1 g/L of Calcofluor White (MilliporeSigma, 18909-
190 100ML-F) for 10 minutes. Following staining, cells were washed with 500µL PBS three times and
191 resuspended in 500µL PBS. Samples were analyzed on a LSRFortessa Flow Cytometer (BD
192 Bioscience, NJ, USA) using BD FACSDiva Software. 10,000 events were recorded for each
193 sample. FlowJo software was used to determine mean fluorescence intensity.

194

195 **Acknowledgements**

196 We thank Joel Whitfield of the University of Michigan Cancer Center Immunology Core and Emma
197 Snyder-White of the University of Michigan Orthopaedic Research Laboratories Histology Core
198 (NIH P30 AR069620) for guidance and technical support for ELISA and histological analysis, and
199 members of the O'Meara lab for discussion. This work was supported by National Institutes of
200 Health grants U19AI181767 and the Burroughs Wellcome Fund Investigators in Pathogenesis
201 award 1173374 to TRO.

202

203 **REFERENCES**

204 1. Ortiz-Roa C, Valderrama-Rios MC, Sierra-Umaña SF, Rodríguez JY, Muñetón-López GA,
205 Solórzano-Ramos CA, Escandón P, Alvarez-Moreno CA, Cortés JA. 2023. Mortality caused
206 by Candida auris bloodstream infections in comparison with other Candida species, a
207 multicentre retrospective cohort. J Fungi (Basel) 9.

208 2. Kim HY PhD, Nguyen TA MSc, Kidd S PhD, Chambers J MD, Alastruey-Izquierdo A PhD,
209 Shin J-H MD, Dao A PhD, Forastiero A MD, Wahyuningsih R MD, Chakrabarti A MD, Beyer
210 P, Gigante V PhD, Beardsley J PhD, Sati H PhD, Morrissey CO PhD, Alffenaar J-W PhD.
211 2024. Candida auris-a systematic review to inform the world health organization fungal
212 priority pathogens list. Med Mycol 62.

213 3. Wang Y, Zou Y, Chen X, Li H, Yin Z, Zhang B, Xu Y, Zhang Y, Zhang R, Huang X, Yang W,
214 Xu C, Jiang T, Tang Q, Zhou Z, Ji Y, Liu Y, Hu L, Zhou J, Zhou Y, Zhao J, Liu N, Huang G,
215 Chang H, Fang W, Chen C, Zhou D. 2022. Innate immune responses against the fungal
216 pathogen Candida auris. Nat Commun 13:3553.

217 4. Xin H, Mohiuddin F, Tran J, Adams A, Eberle K. 2019. Experimental mouse models of
218 disseminated Candida auris infection. mSphere 4.

219 5. Eix EF, Nett JE. 2025. Candida auris: Epidemiology and antifungal strategy. Annu Rev Med
220 76:57–67.

221 6. Santana DJ, Anku JAE, Zhao G, Zarnowski R, Johnson CJ, Hautau H, Visser ND, Ibrahim
222 AS, Andes D, Nett JE, Singh S, O'Meara TR. 2023. A Candida auris-specific adhesin, Scf1,
223 governs surface association, colonization, and virulence. Science 381:1461–1467.

224 7. Iyer KR, Camara K, Daniel-Ivad M, Trilles R, Pimentel-Elardo SM, Fossen JL, Marchillo K,
225 Liu Z, Singh S, Muñoz JF, Kim SH, Porco JA Jr, Cuomo CA, Williams NS, Ibrahim AS,

226 Edwards JE Jr, Andes DR, Nodwell JR, Brown LE, Whitesell L, Robbins N, Cowen LE. 2020.
227 An oxindole efflux inhibitor potentiates azoles and impairs virulence in the fungal pathogen
228 Candida auris. Nat Commun 11:6429.

229 8. Singh S, Uppuluri P, Mamouei Z, Alqarihi A, Elhassan H, French S, Lockhart SR, Chiller T,
230 Edwards JE Jr, Ibrahim AS. 2019. The NDV-3A vaccine protects mice from multidrug resistant
231 Candida auris infection. PLoS Pathog 15:e1007460.

232 9. Zhao G, Lyu J, Veniaminova NA, Zarnowski R, Mattos E, Johnson CJ, Quintanilla D, Hautau
233 H, Hold LA, Xu B, Anku JAE, Steltzer SS, Dasgupta K, Santana DJ, Ibrahim A, Andes D, Nett
234 JE, Singh S, Abraham AC, Killian ML, Kahlenberg JM, Wong SY, O'Meara TR. 2025. *Candida*
235 *auris*skin colonization is mediated by Als4112 and interactions with host extracellular matrix
236 proteins. bioRxiv.

237 10. Herrada J, Roberts K, Gamal A, Long L, Ghannoum MA. 2022. An immunocompromised
238 mouse model of Candida auris systemic infection. Methods Mol Biol 2517:317–328.

239 11. Torres SR, Pichowicz A, Torres-Velez F, Song R, Singh N, Lasek-Nesselquist E, De Jesus M.
240 2020. Impact of Candida auris Infection in a Neutropenic Murine Model. Antimicrob Agents
241 Chemother 64.

242 12. Fakhim H, Vaezi A, Dannaoui E, Chowdhary A, Nasiry D, Faeli L, Meis JF, Badali H. 2018.
243 Comparative virulence of Candida auris with Candida haemulonii, Candida glabrata and
244 Candida albicans in a murine model. Mycoses 61:377–382.

245 13. Wang X, Bing J, Zheng Q, Zhang F, Liu J, Yue H, Tao L, Du H, Wang Y, Wang H, Huang G.
246 2018. The first isolate of Candida auris in China: clinical and biological aspects. Emerg
247 Microbes Infect 7:93.

248 14. Hammer BK, Swanson MS. 1999. Co-ordination of legionella pneumophila virulence with
249 entry into stationary phase by ppGpp. Mol Microbiol 33:721–731.

250 15. Roop RM 2nd, Gee JM, Robertson GT, Richardson JM, Ng W-L, Winkler ME. 2003. Brucella
251 stationary-phase gene expression and virulence. Annu Rev Microbiol 57:57–76.

252 16. Wilson JA, Gulig PA. 1998. Regulation of the spvR gene of the Salmonella typhimurium
253 virulence plasmid during exponential-phase growth in intracellular salts medium and at
254 stationary phase in L broth. Microbiology 144 (Pt 7):1823–1833.

255 17. Ribardo DA, McIver KS. 2003. amrA encodes a putative membrane protein necessary for
256 maximal exponential phase expression of the Mga virulence regulon in Streptococcus
257 pyogenes: Exponential phase expression of Mga. Mol Microbiol 50:673–685.

258 18. Levi M, van der Poll T. 2017. Coagulation and sepsis. Thromb Res 149:38–44.

259 19. Litvinov RI, Pieters M, de Lange-Loots Z, Weisel JW. 2021. Fibrinogen and fibrin. Subcell
260 Biochem 96:471–501.

261 20. Gulla KC, Gupta K, Krarup A, Gal P, Schwaeble WJ, Sim RB, O'Connor CD, Hajela K. 2010.
262 Activation of mannan-binding lectin-associated serine proteases leads to generation of a
263 fibrin clot: MASPs generate a fibrin clot. Immunology 129:482–495.

264

265

266

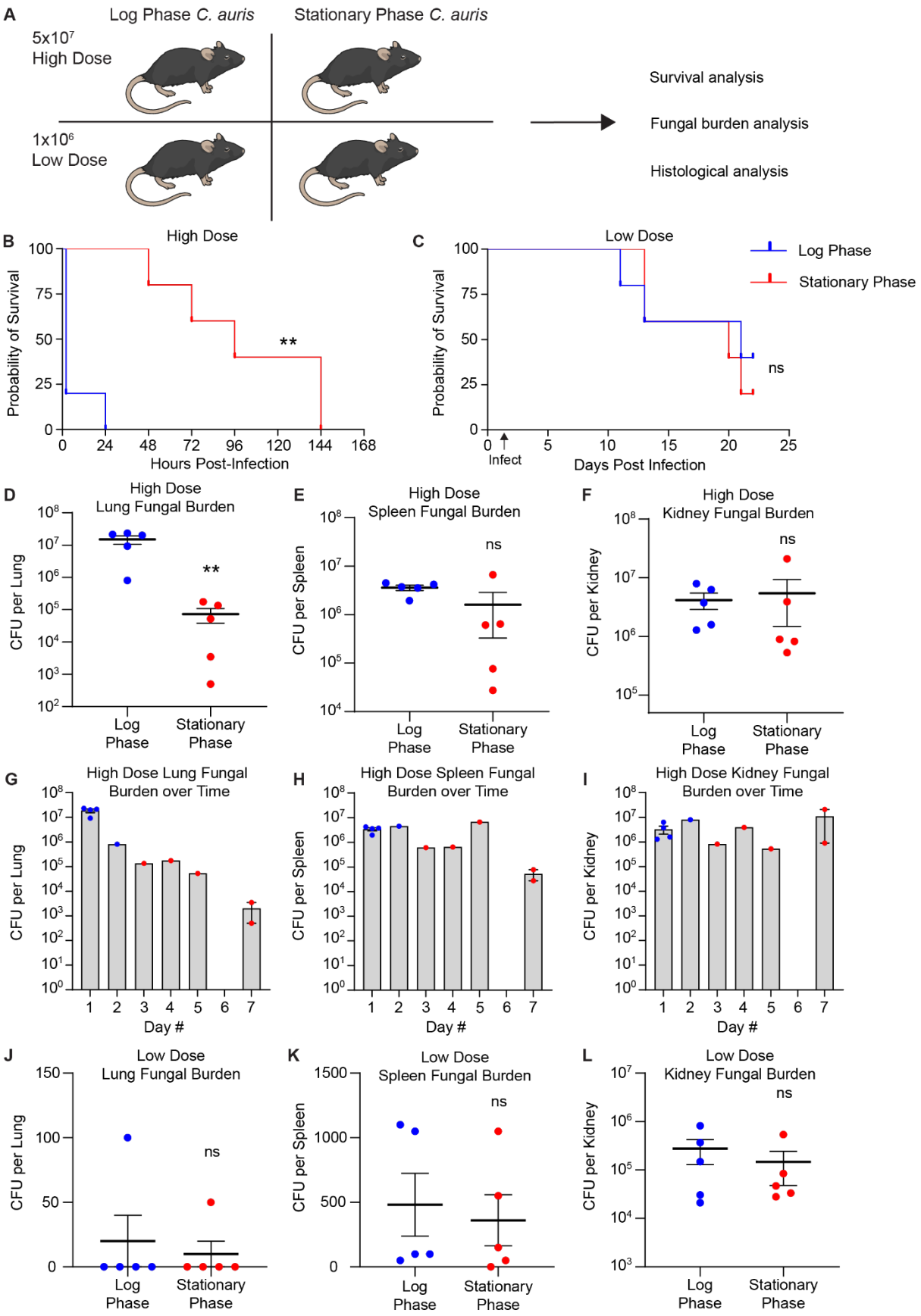
A
Log Phase C. auris
Stationary Phase C. auris
5x10⁷
High Dose
1x10⁶
Low Dose
Survival analysis
Fungal burden analysis
Histological analysis
B
High Dose
Probability of Survival
Hours Post-Infection
**
C
Low Dose
Log Phase
Stationary Phase
ns
Infect
Days Post Infection
D
High Dose
Lung Fungal Burden
CFU per Lung
E
High Dose
Spleen Fungal Burden
CFU per Spleen
F
High Dose
Kidney Fungal Burden
CFU per Kidney
G
High Dose Lung Fungal Burden over Time
H
High Dose Spleen Fungal Burden over Time
I
High Dose Kidney Fungal Burden over Time
Day #
J
Low Dose
Lung Fungal Burden
K
Low Dose
Spleen Fungal Burden
L
Low Dose
Kidney Fungal Burden
Log Phase
Stationary Phase

267

268 **Figure 1: *Candida auris* growth phase influences survival kinetics after systemic infection.**
269 **(A)** Experimental scheme: Immunocompetent C57BL/6J mice (n=5 per cohort) were infected with
270 a high dose ($5x10^7$) or low dose ($1x10^6$) of B11109 *C. auris* in log phase or stationary phase
271 growth, and survival was monitored. Fungal burden and histological analysis were performed in
272 select organs post-mortality. **(B-C)** Survival probability plots comparing log and stationary phase
273 high dose *C. auris* infection (B) or low dose *C. auris* infection (C). **(D-F)** Post-mortality fungal
274 burden analysis from lung (D), spleen (E), or kidney samples (F) in high dose cohorts. **(G-I)** Post-
275 mortality fungal burden analysis from lung (G), spleen (H), or kidney samples (I) in high dose
276 cohorts plotted as a function of time. Blue dots represent the log phase-infected cohort and red
277 dots represent the stationary phase-infected cohort. **(J-L)** Post-mortality fungal burden analysis
278 from lung (J), spleen (K), or kidney samples (L) in low dose cohorts. * $p<0.05$, ** $p<0.01$, ns not
279 significant by Mantel-Cox test (B-C) or Student's unpaired t test (E-F, J-L).

280

281

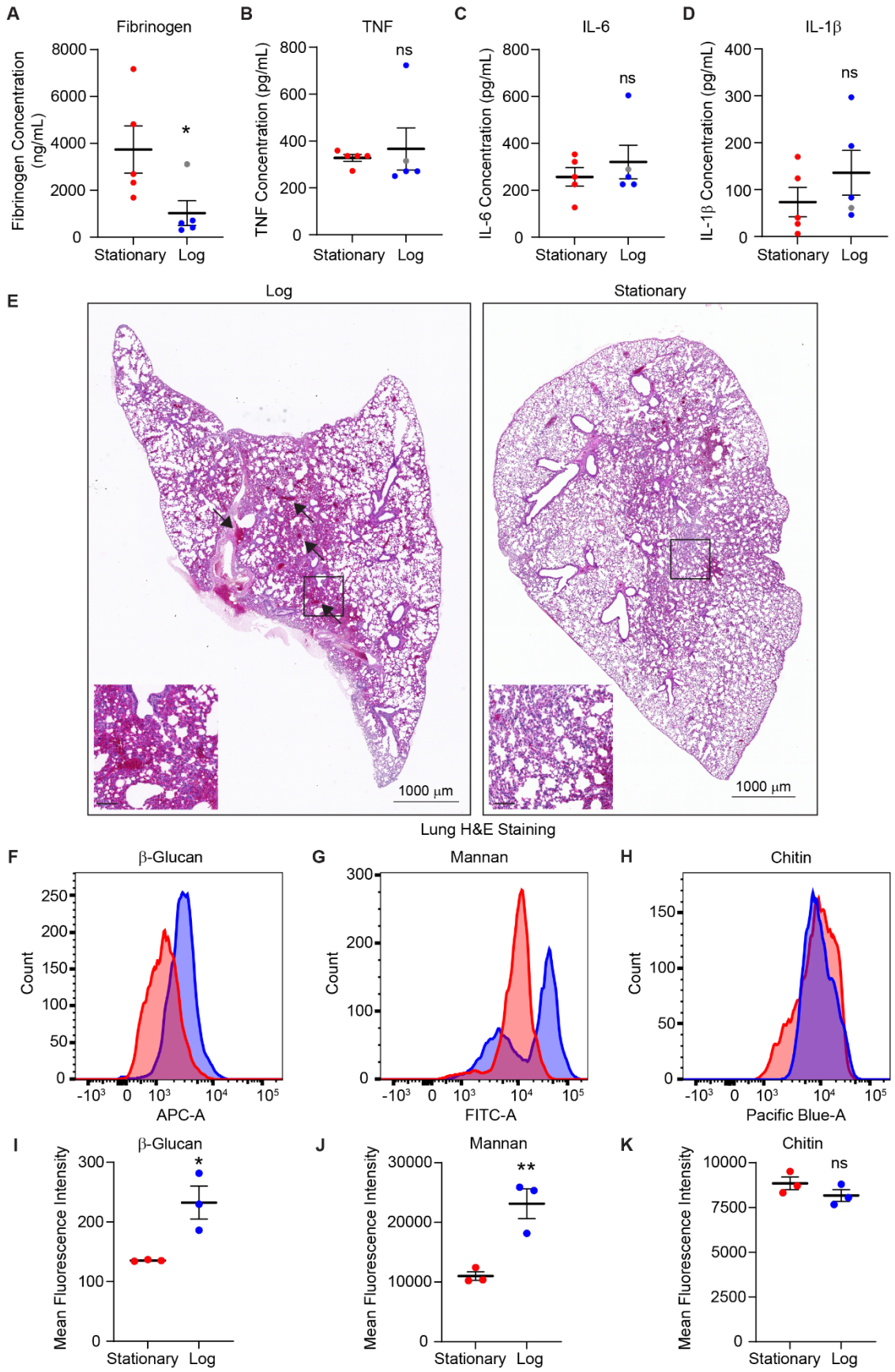
A
Fibrinogen
Fibrinogen Concentration (ng/mL)
8000
6000
4000
2000
0
*
Stationary
Log
B
TNF
TNF Concentration (pg/mL)
800
600
400
200
0
ns
Stationary
Log
C
IL-6
IL-6 Concentration (pg/mL)
800
600
400
200
0
ns
Stationary
Log
D
IL-1β
IL-1β Concentration (pg/mL)
400
300
200
100
0
ns
Stationary
Log
E
Log
Stationary
1000 μm
1000 μm
Lung H&E Staining
F
β-Glucan
Count
250
200
150
100
50
0
-10³
0
10³
10⁴
10⁵
APC-A
G
Mannan
Count
300
200
100
0
-10³
0
10³
10⁴
10⁵
FITC-A
H
Chitin
Count
150
100
50
0
-10³
0
10³
10⁴
10⁵
Pacific Blue-A
I
β-Glucan
Mean Fluorescence Intensity
300
200
100
0
*
Stationary
Log
J
Mannan
Mean Fluorescence Intensity
30000
20000
10000
0
**
Stationary
Log
K
Chitin
Mean Fluorescence Intensity
10000
7500
5000
2500
0
ns
Stationary
Log

282

283 **Figure 2: Systemic infection with log phase *Candida auris* at high dose triggers rapid blood**
284 **clotting. (A-D)** ELISA data showing levels of Fibrinogen (A), TNF (B), IL-6 (C), and IL-1β (D) from
285 mouse plasma samples harvested post-mortality. Gray data point denotes the mouse within the
286 log phase high dose cohort that survived until day 1 post-infection. **(E)** Representative
287 hematoxylin and eosin (H&E) staining of lung sections from mice in high dose cohorts infected
288 with log phase (left) or stationary phase (right) *C. auris*. Arrows denote blood clots in the lung.
289 Boxes show a magnified inset (scale bar 100 μm). **(F-H)** Representative plots from flow cytometry
290 analysis of *C. auris* cell wall components: β-glucan (measured by human Dectin-1 binding),
291 mannan (measured with concanavalin A-FITC), and chitin (measured with calcofluor white). **(I-K)**
292 Quantification of mean fluorescence intensity of cell wall component staining from flow cytometry
293 analysis, as in F-H: β-glucan (I), mannan (J), and chitin (K). * $p<0.05$, ** $p<0.01$, ns not significant
294 by Student's unpaired t test.

295